DATA ANALYTICS AND APPLIED MATHEMATICS (DAAM)
e-ISSN: 2773-4854
VOL. 2, ISSUE 2, 001 – 013
DOI: https://doi.org/10.15282/daam.v2i2.6831

ORIGINAL ARTICLE

Shape effect of Cu, Al_2O_3 and TiO_2 nanoparticles on stagnation point nanofluid flow in a microgravity environment environment

M.H.A. Kamal[1], A. Ali[1], Y.J. Lim[1], N.A. Rawi[1] and S. Shafie[1,*]

[1]Department of Mathematical Sciences, Faculty of Science, Universiti Teknologi Malaysia, UTM Johor Bahru, 81310 Johor Bahru, Johor Darul Takzim, Malaysia.

ABSTRACT – The unsteady viscous nanofluid flow near a three-dimensional stagnation point was studied numerically under microgravity environment. g-Jitter is one of the effects occurs under microgravity environment that producing a fluctuating gravitational field. Three different types of nanoparticles were induced in the study that is copper (Cu), alumina (Al_2O_3), and titania (TiO_2) which then produce a water-based typed of nanofluid. In addition, different shape of nanoparticle was applied on the study in analyzing the performance of each types of nanoparticle. The fluid system was then mathematically formulated into a system of partial differential equation based on physical law and principle such as conservation of mass, Newton's second law and conservation of energy. The system of equation then undergoes semi-similar transformation technique in reducing the complexity of the problem into non dimensionless form. Keller box method was applied into the dimensionless system of equations in solving the problem numerically. The problem was analyzed in term of velocity and temperature profiles together with skin friction coefficient and Nusselt number. The results shown that temperature profile, skin friction coefficient and Nusselt number were increase while velocity profile decreased as nanoparticle volume fraction decreased. The results indicated that, the needle-shaped nanoparticles give the highest enhancement on the heat transfer of the nanofluid compared to sphere and disk-shaped nanoparticles with more than 14% significant different. In addition, alumina hold the highest velocity profile while copper hold the lowest velocity profile.

ARTICLE HISTORY
Received: 21/08/2021
Revised: 02/10/2021
Accepted: 02/12/2021

KEYWORDS
Boundary layer flow
Nanofluid
Shape effect
Gravity modulation
Stagnation point

INTRODUCTION

In a micro-electromechanical system (MEMS), the low performance of the heat transfer fluid such as oil, diethylene glycol, ethylene glycol, fuels, and water has limited the effectiveness and compactness of the devices. Besides, the highly effective heat transfer fluid is also a substantial part of the transportation industry, industrial processes, food manufacturing, chemical engineering, heat exchangers, electronic cooling, and nuclear reactors. To overcome this shortcoming, many researchers have made an astonishing effort in enhancing the thermal properties of the heat transfer fluid. Generally, the rate of the heat transmission can be improved by suspending solid particles in the thermal system or increasing the fluid flow, or extending the surface by adding wavy, plain, perforated, pin, louvered, and offset strip. Maxwell et al. [1] primarily developed a theoretical study on the thermal conductivity of solid-liquid mixtures by considering solid particles in the size of a micrometer and/or millimeter. The thermal properties of the fluids were observed to be increased. However, problems such as increment of pressure drop, erosion, fouling, agglomeration, clogging, and sedimentation were detected in those fluids. These obstacles have encouraged researchers to explore the use of nanoparticles. In view of this, Choi [2] experimented thermal behavior of the fluid that was suspended by nanoparticles and then introduced the term of nanofluid to define such kind of fluid. Further, Choi et al. [3] noticed that the thermal conductivity of the traditional heat transfer fluid was enhanced approximately twice when <1% of nanoparticles were added into the fluid.

Khanafer et al. [4], Tiwari and Das [5] have scrutinized the heat transfer performance of a nanofluid in a square cavity. Khanafer et al. [4] had concerned the fluid flow that was driven by a buoyancy force and on the other hand, the fluid flow induced by a two-sided lid was elucidated by Tiwari and Das [5]. In both investigations, the authors observed that the suspended nanoparticles do enhance the rate of heat transport in the fluid. Besides, the presented results have indicated that the rate has an increasing behavior with the volume fraction of the nanoparticles. The thermal properties of the nanofluid change with variation of size, shape, volume fraction, base fluid, and type of the nanoparticle [6-14]. Jmai et al. [6] have deliberated the effect of the different types of nanoparticles which are Cu, silver (Ag), Al_2O_3, and TiO_2 on the heat enhancement of the fluid flow in an enclosure cavity with two partially heated sidewalls. The authors found that the Cu–water nanofluid has promised a higher heat transfer rate than the Al_2O_3–water, and TiO_2–water nanofluids. The heat analysis for four different types of nanoparticles in a squeezing flow along with two rotating parallel plates with a stretching lower plate has been acknowledged by Zubair et al. [7]. The study has shown that the four different nanofluids

*CORRESPONDING AUTHOR | S. Shafie | ✉ sharidan@utm.my

have the same response for the variation of the pertinent parameters. However, a different magnitude of the velocity and temperature profile was provided when a different type of nanoparticle has been utilized. This indicates that the type of the utilized nanoparticle in the fluid has altered the distribution of the fluid fields but does not change the behavior of the fluid due to the various physical parameters. Further discussion on the effect of the type of nanoparticle can be obtained by Hajabdollahi et al. [8] and Javadi et al. [9].

The influence of the nanoparticle shape such as bricks, platelets, blades, and cylindrical on the performance of a heat exchanger was theoretically discussed by Elias at al. [10]. The nanofluid with cylindrical nanoparticles was found to has a better thermal property as compared with the other shape. Moreover, the nanofluid with nanoparticles in the shape of blade and platelet has shown a weaker overall heat transfer rate. However, Sheikholeslami and Bhatti [11] had illustrated that the platelet shape has the greatest heat transfer coefficient for a nanofluid flow in a semi-annulus with porous media. Further, Khan [13] concluded that the molybdenum disulphide (MoS_2) nanoparticle with the shape of a blade has the highest heat transport rate for a mixed convection nanofluid flow in a vertical channel under the influence of a porous medium. Different observation has been recognized regarding the effect of the nanoparticle shape, this possible because of the type of the applied nanoparticle and the base fluid. As stated by Zakari et al. [14] that the nature of the base fluid and also the nanoparticle are significantly enhancing or diminishing the convection of the temperature in the fluid.

Besides, some researchers have examined the nanofluid under various situations. Analysis of the stagnation point nanofluid flow is essential in practical application and also in the fundamental theory of fluid mechanics. Such kind of fluid has existed in many manufacturing processes and engineering industries, for example; food processing, petrochemical industries, paper production, oil recovery, glass fiber production, and polymer extrusion. Bachok et al. [15] discussed the effect of the three-dimensional stagnation point on the fluid field and heat transfer, respectively, of three different kinds of nanofluid which are Cu-water, Al_2O_3-water, and TiO_2-water. The authors found the stagnation point has enhanced the velocity profiles but a reverse trend was detected in the temperature curve. Further, the highest coefficient of the heat transfer was revealed by the Cu-nanofluid. Further, Mustafa et al. [16] have deliberated the stagnation point nanofluid flow over a stretching sheet. Then, the effect of the Navier's slip velocity and stagnation point on the nanofluid flow toward a stretching horizontal plate has been acknowledged by Malvandi et al. [17]. More interesting research about the stagnation point nanofluid flow is illustrated by Hayat et al. [18] and Soomro et al. [19].

On the other hand, the gravity modulation effect or more well known as the g-jitter effect has been considered by some investigators on the velocity and temperature distribution of a nanofluid [20-24]. The g-jitter effect is only be detected when the microgravity environment is concerned. It is a consequence of the orbiter maneuvers, vibrations of the equipment, crew activities, gradient of the earth's gravity, and the drag of the solar. Uddin et al. [20] had studied the mixed convection and heat transfer of a nanofluid over a moving sheet under the influence of g-jitter and convective heat flux. Moreover, the diffusion of the concentration of the nanoparticles in the fluid due to the concentration gradient has been taken into account by the authors. The obtained result showed that the gravity modulation has increased the transformation of the heat. Recently, Kamal et al. [24] analyzed the nanofluid flow under the effect of three-dimensional stagnation point of a body, heat generation, and g-jitter. The authors concluded that the stagnation point has a dominant impact on the fluid velocity but the heat and mass transfer in the fluid were significantly affected by the g-jitter. Then, Kamal et al. [24] extended their work before as discussed in [23] by considering the influence of thermal radiation.

In view of the above literature survey, there is no report available about the effect of the shape, and type of nanoparticles on the enhancement of the heat performance for a nanofluid flow near a three-dimensional stagnation point with the influence of gravity modulation. Therefore, the present study aims to elucidate the distribution of the velocity and temperature of a stagnation point nanofluid flow that is induced by the g-jitter effect for three different shapes and types of nanoparticles by intoducing a mathematical model that represent the flow behaviour . Cu-water, Al_2O_3-water, and TiO_2-water nanofluid have been considered in the present communication. The impact of three different shapes which are cylindrical, spherical, and blade of each type of nanoparticle on the fluid field is displayed graphically and analyzed. Initially, the flow problem is mathematically modeled together with certain concerning no-slip boundary conditions. Suitable dimensionless variables are then utilized to convert the partial governing equations into ordinary differential equations. Subsequently, the Keller box method is applied to determine the numerical solutions. The fluid behavior and thermal properties of the nanofluid due to the variation of the pertinent parameters are discussed through graphs and tables.

MATHEMATICAL FORMULATION

Consider viscous boundary layer nanofluid flow near a three dimensional stagnation point influenced by g-jitter effect is studied. No slip boundary condition with constant wall temperature was applied on the fluid system. Three different types of water base of nanofluid as induced together with different shape of nanoparticle. Nodal point of attachment **N**, represent the location of stagnation point that located at the origin of three dimensional ortogonal Cartesian coordinate system (x, y, z). The $x-$ and $y-$ coordinates were measured along the body of the surface while the $z-$ coordinate was measured normal to the body. The physical model of the fluid system is presented in Figure 1.

The g-jitter effect that produced a fluctuation gravitational field behaviour depent on time t, defined as,

$$g(t) = g_0\left[1 + \varepsilon\cos\left(\pi\omega t\right)\right] \tag{1}$$

where g_0 represent mean of gravity acceleration, ε is amplitude of modulation and ω is frequency of oscillation. The system of equation is simplfied by using boundary layer and Boussinesq approximation subjected to effect considered. Thus, the system of equation becomes,

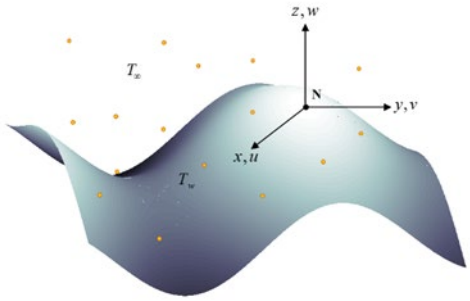

Figure 1. Physical model.

$$\frac{\partial u}{\partial x}+\frac{\partial u}{\partial y}+\frac{\partial u}{\partial z}=0, \tag{2}$$

$$\rho_{nf}\left(\frac{\partial u}{\partial t}+u\frac{\partial u}{\partial x}+v\frac{\partial u}{\partial y}+w\frac{\partial u}{\partial z}\right)=\mu_{nf}\frac{\partial^2 u}{\partial z^2}+g(t)(\rho\beta)_{nf}\,ax\left(T-T_\infty\right), \tag{3}$$

$$\rho_{nf}\left(\frac{\partial v}{\partial t}+u\frac{\partial v}{\partial x}+v\frac{\partial v}{\partial y}+w\frac{\partial v}{\partial z}\right)=\mu_{nf}\frac{\partial^2 v}{\partial z^2}+g(t)(\rho\beta)_{nf}\,by\left(T-T_\infty\right), \tag{4}$$

$$\frac{\partial T}{\partial t}+u\frac{\partial T}{\partial x}+v\frac{\partial T}{\partial y}+w\frac{\partial T}{\partial z}=\alpha_{nf}\frac{\partial^2 T}{\partial z^2}, \tag{5}$$

subjected

$$\begin{aligned} &t<0: u=v=w=0, T=T_\infty \text{ for any } x, y \text{ and } z,\\ &t\geq 0: u=v=w=0, T=T_w \text{ on } z=0, x\geq 0, y\geq 0,\\ &\quad u=v=w=0, T=T_\infty \text{ as } z\to 0, x\geq 0, y\geq 0. \end{aligned} \tag{6}$$

Parameter u,v and w are the velocity component along the direction x,y,z axes respectively with T is the temperature parameter. The subscription nf represents nanofuid where thermophysical propertise ρ,μ,β and α denote the density, dynamic viscosity, thermal expansion and thermal diffusion. The principal curvature was presented by notion a and b which holds propertise such that $|a|\geq|b|$ with $a>0$ and $c=b/a$. Here, c is defined as curvature ratio at **N**, by taking a positive value with a range of $0\leq c\leq 1$. By using semi-similar transformation technique, the complexity of the problem is reduced. The semi-similar variables are introduced such that [25],

$$\begin{aligned} &\eta=Gr^{1/4}az,\quad \tau=\Omega t,\quad t=\upsilon a^2 Gr^{1/2}t^*,\\ &u=\upsilon a^2 xGr^{1/2}f',\quad v=\upsilon a^2 yGr^{1/2}h',\quad w=-\upsilon aGr^{1/4}\left(f+h\right),\\ &\Omega=\frac{\omega}{\upsilon a^2 Gr^{1/2}},\quad \theta=\frac{\left(T-T_\infty\right)}{\left(T_w-T_\infty\right)},\quad Gr=\frac{g_0\beta\left(T-T_\infty\right)}{a^3\upsilon^2}, \end{aligned} \tag{7}$$

where η is boundary layer thickness and Gr is the Grashof number. Ω and θ is the dimensinless parameter of frequency of oscillation and temperature. Since the nanofluid model applied in this study focussing on heat transfer performance, the nanofluid correlation was introduced derived from the Maxwell and Brinkman model that defined as [26],

$$\begin{aligned} &\alpha_{nf}=\frac{k_{nf}}{\left(\rho C_p\right)_{nf}},\\ &\rho_{nf}=(1-\phi)\rho_f+\phi\rho_s,\quad (\rho\beta)_{nf}=(1-\phi)(\rho\beta)_f+\phi(\rho\beta)_s,\\ &\left(\rho C_p\right)_{nf}=(1-\phi)\left(\rho C_p\right)_f+\phi\left(\rho C_p\right)_s. \end{aligned} \tag{8}$$

The subscript f and s represent the fluid and solid component in the nanofluid mixture respectively while k is the thermal conductivity. On the other hand, the effective dynamic viscosity is defined as [27],

$$\mu_{nf} = \mu_f \left(1 + p\phi + q\phi^2\right) \tag{9}$$

where the constant values of p and q are depended on the particle shape as given in Table 1 and μ_f is the dynamic viscosity of the base fluid [27], [28].

Table 1. Empirical value of shape factor parameter.

Model	Sphere	Cylinder (needle-shaped)	Blade (disk-shaped)
p	2.5	13.5	14.6
q	6.2	904.4	123.3

Next, the thermal conductivity taken a form such that,

$$\frac{k_{nf}}{k_f} = \frac{k_s + (n-1)k_f - (n-1)(k_f - k_s)\phi}{k_s + (n-1)k_f + (k_f - k_s)\phi}, \tag{10}$$

with n as the empirical shape factor given by

$$n = \frac{3}{\psi^*} \tag{11}$$

where ψ^* is the sphericity defined as the ratio between the surface area of the sphere and surface area of the real particle with equal volumes. Following Timofeeva et al. [28], the values of ψ^* for different shape particles are given in Table 2.

Table 2. Sphericity for different shapes of nanoparticles.

Model	Sphere	Cylinder (needle-shaped)	Blade (disk-shaped)
ψ^*	1	0.62	0.36

Present study applied three different types of nanoparticle which are copper, alumina and titania. The thermophysical properties of copper, alumina, titania and water are shown in Table 3 [6], [29],

Table 3. Thermophysical of the nanoparticles and base fluid.

Physical Properties	Water	Copper	Alumina	Titania
Density	997.1	8933	3970	4250
Specific heat capacity	4179	385	765	686.2
Thermal conductivity	0.613	401	40	8.9538
Thermal expension	21	1.67	0.85	0.9

By using all information in (7) – (11), semi-similar transformation technique was performed. The dimensionless system of equation written as,

$$C_1 f''' + C_2 (f + h) f'' - C_2 f'^2 + C_3 \left[1 + \varepsilon \cos(\pi\tau)\right]\theta = C_2 \Omega \frac{\partial f'}{\partial \tau}, \tag{12}$$

$$C_1 h''' + C_2 (f + h) h'' - C_2 h'^2 + cC_3 \left[1 + \varepsilon \cos(\pi\tau)\right]\theta = C_2 \Omega \frac{\partial h'}{\partial \tau}, \tag{13}$$

$$\frac{C_4}{C_5 \,\mathrm{Pr}} \theta'' + (f + h)\theta' = \Omega \frac{\partial \theta}{\partial \tau}, \tag{14}$$

where Pr is Prandtl number while C1,C2,C3,C4 and C5 is a constant defined as,

$$C_1 = \left(1 + p\phi + q\phi^2\right), \quad C_2 = 1 - \phi + \frac{\phi\rho_s}{\rho_f}, \quad C_3 = 1 - \phi + \frac{\phi(\rho\beta)_s}{(\rho\beta)_f},$$
$$C_4 = \frac{k_{nf}}{k_f}, \quad C_5 = 1 - \phi + \frac{\phi(\rho C_p)_s}{(\rho C_p)_f}. \tag{15}$$

subjected to dimensionless boundary condition

$$f(\eta,0) = f'(\eta,0) = 0, \quad h(\eta,0) = h'(\eta,0) = 0, \quad \theta(\eta,0) = 1,$$
$$f' \to 0, \quad h' \to 0, \quad \theta \to 0, \quad \text{as } \eta \to \infty. \tag{16}$$

The dimensionless system of equation was solved numerically using Keller box method and analysed subjected to velocity and temperature profiles, skin friction coefficient together with Nusselt number.

RESULTS AND DISCUSSION

The dimensionless system of equation (12) – (16) was solved numerically using finite different approach known as Keller box method. The flow problem was analysed in term of profiles and physical quantities subjected to effect considered such as nanoparticle volume fraction ϕ, types of nanoparticle and shape of the nanoparticle. Comparison study was conducted with previous published results to measure the accuracy of the method and algorithm applied in solving the system of equations. Table 4 shows the comparison between solutions of Sharidan [30] and the results obtained in the present study with $c = 0.5, \Omega = 0.2, \text{Pr} = 0.72$ and $\phi = 0$. Here f'' and h'' are the skin friction subjected to $x-$ and $y-$direction respectively while θ' is the Nusselt number. The results of the present study are in a very good agreement with the outputs provided in the literature.

Table 4. Results comparison for limited cases in term of skin friction and Nusselt number.

ε	Sharidan [30]			Present		
	f''	h''	θ	f''	h''	θ
0.0	0.7991	0.4266	0.4287	0.7989	0.4264	0.4287
0.2	0.7976	0.4260	0.4280	0.7980	0.4260	0.4280
0.4	0.7940	0.4240	0.4258	0.7946	0.4243	0.4258
0.6	0.7875	0.4207	0.4219	0.7885	0.4212	0.4219
0.8	0.7780	0.4161	0.4160	0.7794	0.4167	0.4160
1.0	0.7652	0.4100	0.4071	0.7669	0.4108	0.4071

Figure 2 shows the velocity and temperature profiles as ϕ parameter increases. A decreasing behavior is shown on the velocity profile while increasing behaviour is shown on temperature profile. The movement of the fluid was slowing down due to the additional of nanoparticle that increase the shear stress on the fluid. On the other hand, the increasing behaviour on the temperature profile is due to the higher thermal propertise hold by the added nanoparticle. The additional of nanoparticle sucessfully enhance the thermal conductivity of the conventional fluid that have low thermal conductivity.

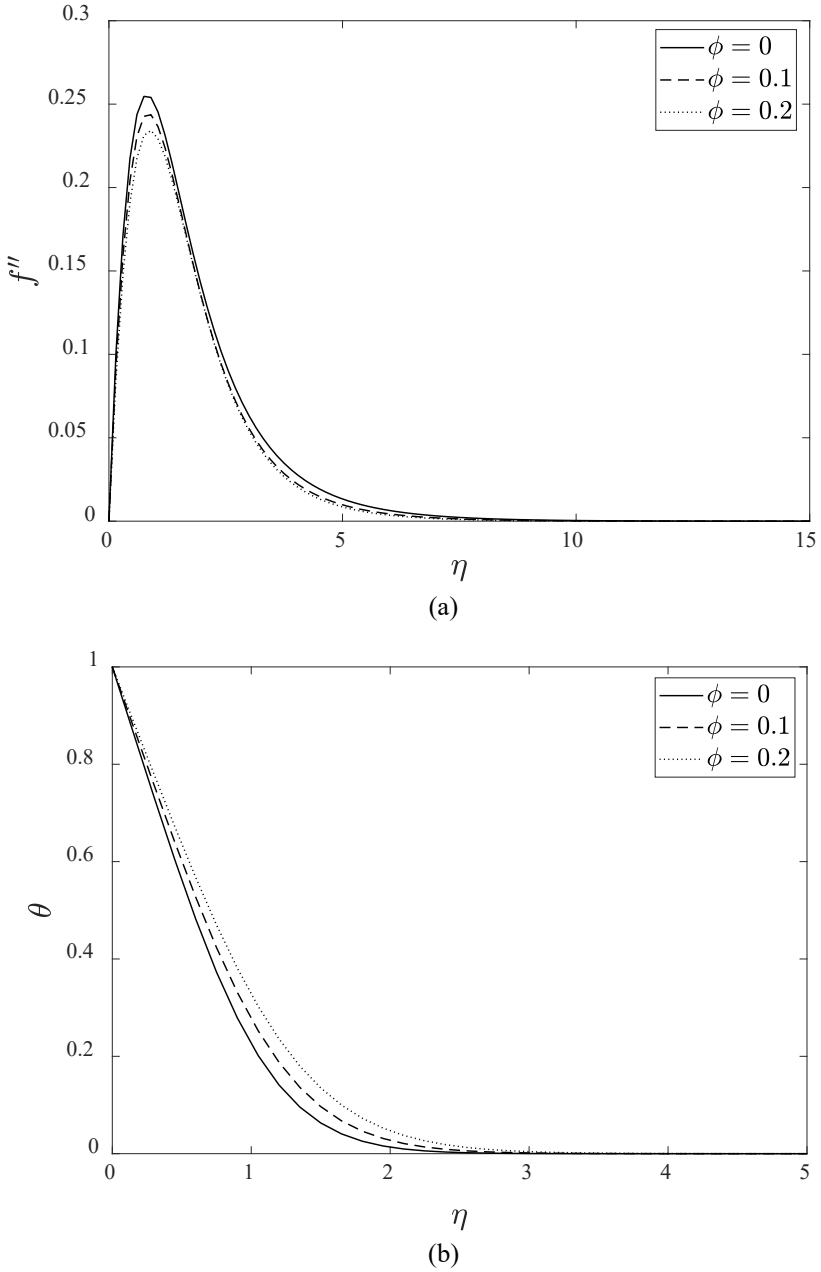

Figure 2. The profiles for various value of nanoparticle volume fraction (a) velocity profile (b) temperature profile.

The effect of nanoparticle volume fraction also analysed in term of skin friction coefficient and Nusselt number as shown in Figure 3. From the figures, increasing of nanoparticle volume fraction increases both skin friction coefficient and Nusselts number. The increases of skin friction coefficient is due to the additional resistance produced by nanoparticle added into the fluid system. Thus, greater skin friction coefficient experienced by the boundary body by increases of the nanoparticle volume fraction. On the other hand, Nusselt number describe the rate of change of heat transfer at the surface of the boundary body. Nusselt number is an indicator that shown an enhancement in term of thermal conductivity at the boundary body as the nanoparticle added into the fluid system. Thus, an enhancement on thermal conductivity succesfully achieved either in the fluid or at the surface of boundary body.

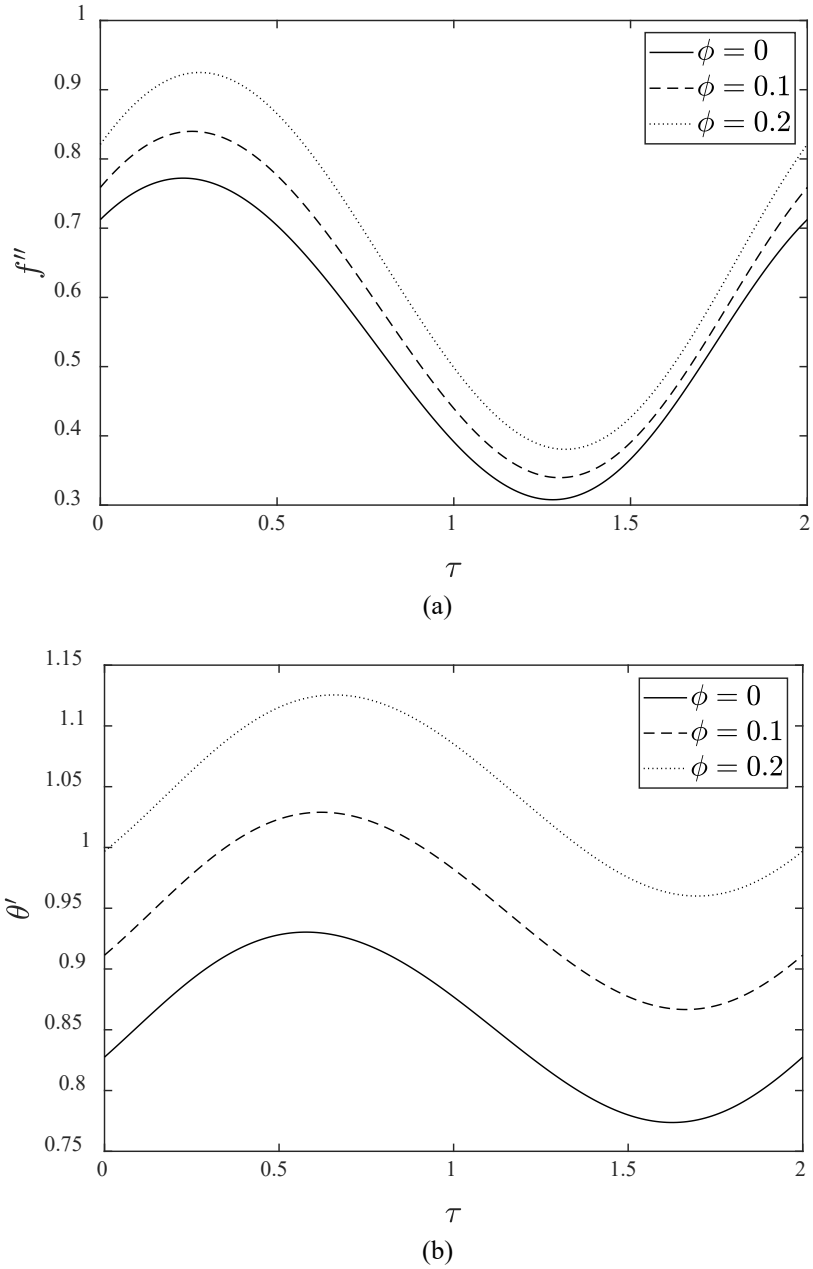

Figure 3. The physical quantities for various value of nanoparticles volume fraction (a) skin friction coefficient (b) Nusselt number.

Figure 4 and Figure 5 on the other hand show the effect of different types of nanoparticle induced on the fluid system in term of profiles, skin friction coefficient and Nusselt number. In this study, copper, alumina and titania nanoparticle was saturated with water as the base fluid in producing the nanofluid. From Figure 4, alumina hold the highest velocity profile while copper hold the lowest velocity profile. Besides that, there is only slightly different on temperature profile for all types of nanofluid considered with copper has the highest temperature profile and titania has the lowest temperature profile. On the other hand, the numerical results on different types of nanoparticles was presented in Figure 5 with variables types of nanoparticle in term of skin friction and Nusselt number. Copper holds the highest for both skin friction and Nusselt number while titania hold the lowest for both physical quantities.

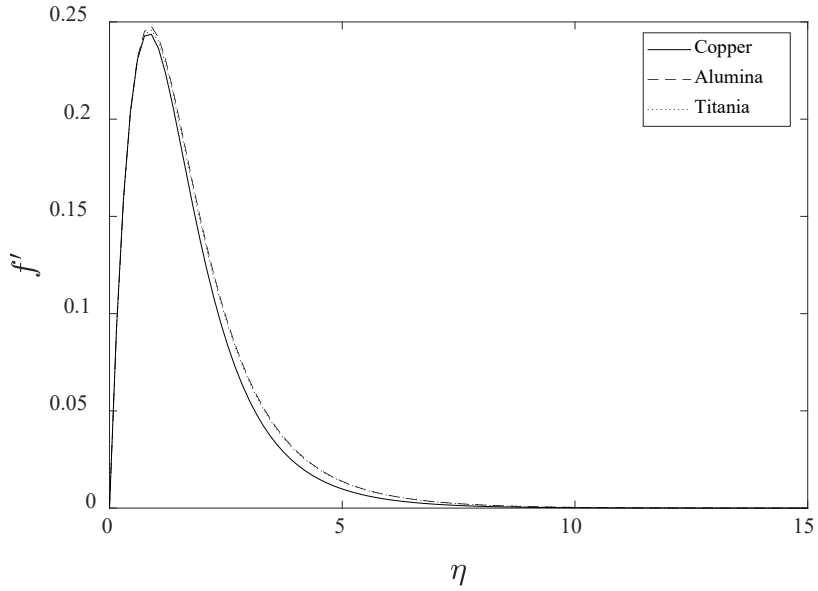

(a)

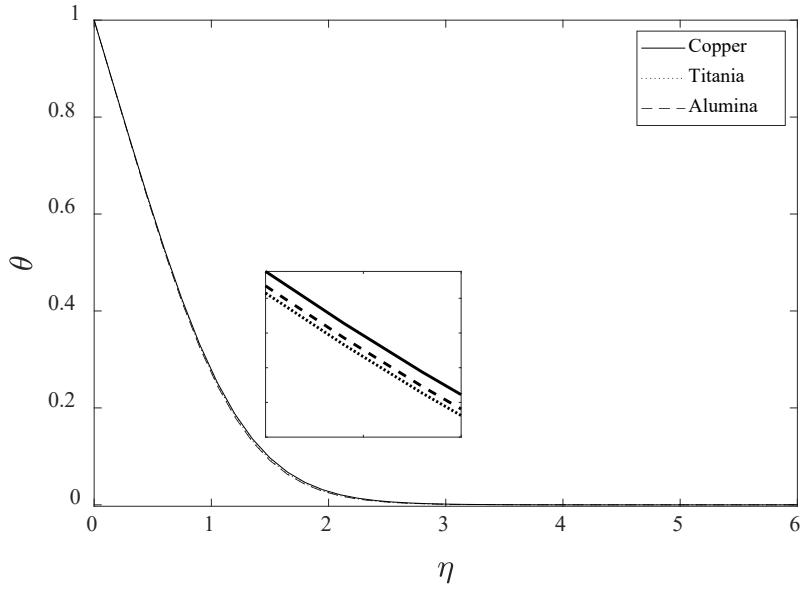

(b)

Figure 4. The profiles for various types of nanoparticles (a) velocity profile (b) temperature profile.

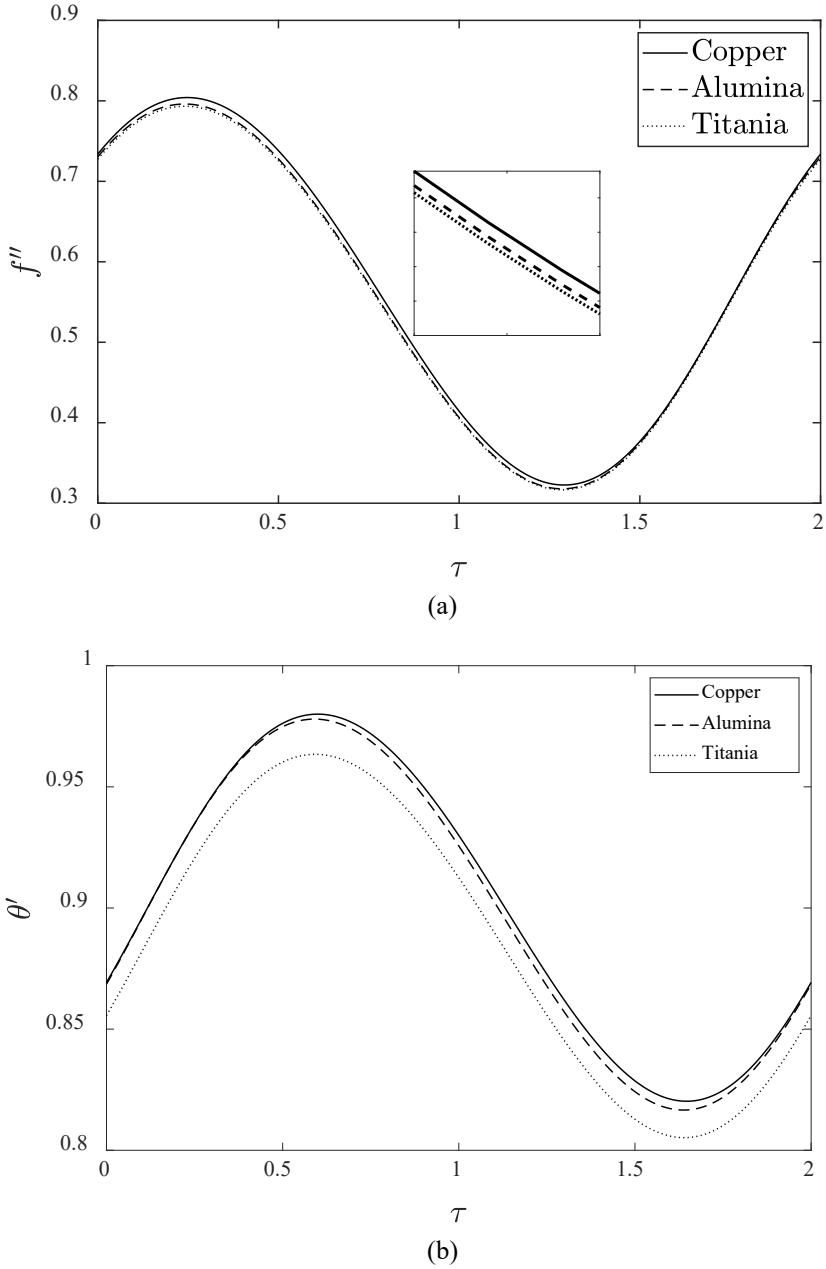

Figure 5. The physical quantities for various types of nanoparticles (a) skin friction coefficient (b) Nusselt number.

Different shape of nanoparticle on the other hand are analysed in Figure 6 and Figure 7 with sphere, blade and cylinder shape of nanoparticles were induced into the system. From Figure 6, by inducing copper as the nanoparticles, sphere shape of nanoparticle achieved the higest velocity profile while blade shape of nanoparticle holds lowest velocity profile. On the other hand, the blade shape of nanoparticles has thicker boundary layer thickness compared with other shape of nanoparticles. Figure 7 on the other hand present the physical quantities analysis with different shape of nanoparticles induced. As for the skin friction coefficent, sphere shape of nanoparticle has the lowest skin friction coefficient while blade has the highest skin friction coefficient. On the other hand, cylinder shape has the highest Nusselt number while blade shape of nanoparticle has the lowest Nusselt number. The analysis on shape factor of nanoparticles was also conducted with diferent types of nanoparticles as shown in Table 5. The behaviour on different shape of nanoparticles was found to be the same regardless type of nanoparticles.

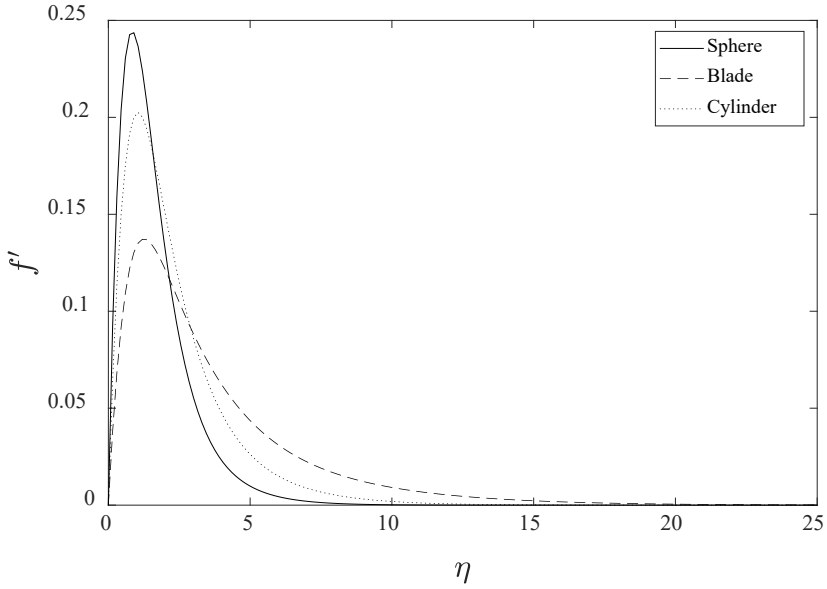

(a)

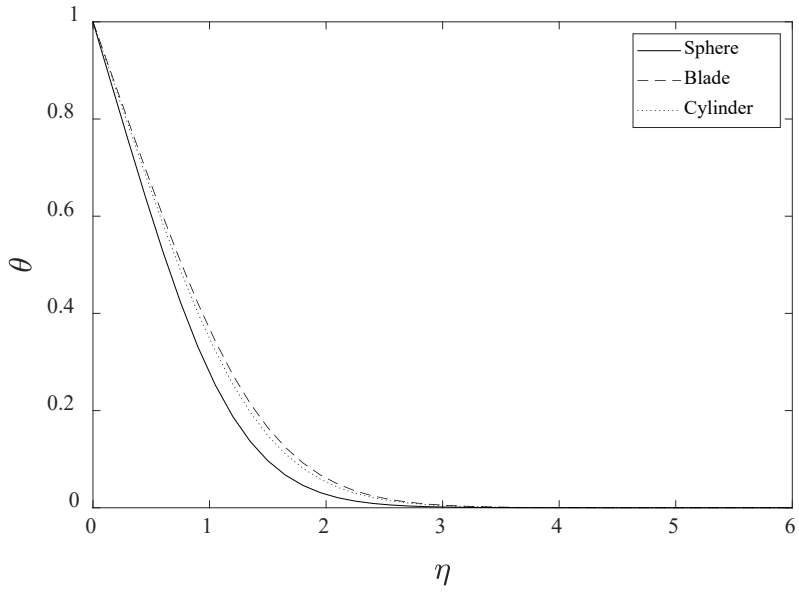

(b)

Figure 6. The profiles for various shape of nanoparticles (a) velocity profile (b) temperature profile.

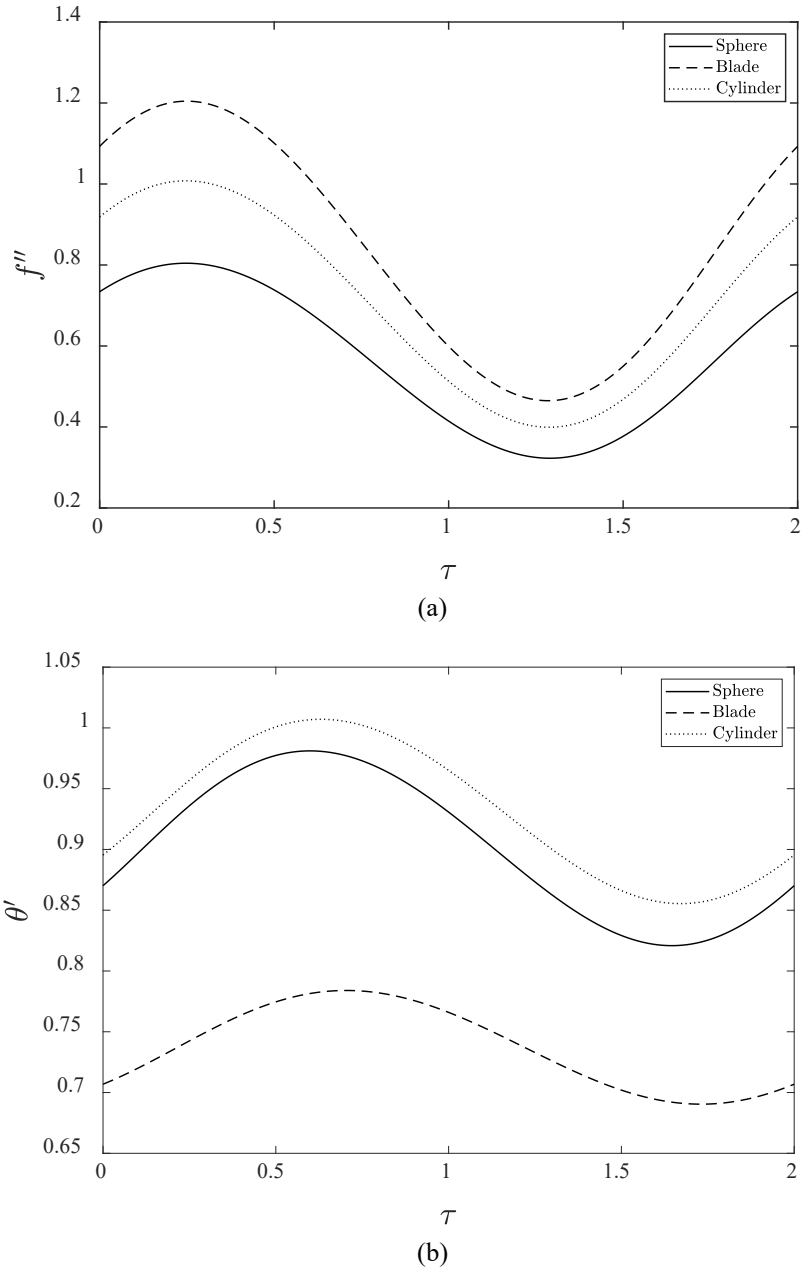

Figure 7. The physical quantities for various shape of nanoparticles (a) skin friction coefficient (b) Nusselt number.

Table 5. Results comparison for limited cases in term of skin friction and Nusselt number.

Shape	Cu		Al_2O_3		TiO_2	
	C_{fx}	Nu	C_{fx}	Nu	C_{fx}	Nu
Sphere	0.5670	0.9027	0.5612	0.9002	0.5593	0.8873
Blade	0.7655	0.9769	0.7503	0.9550	0.7438	0.8959
Cylinder	0.6846	0.8541	0.6716	0.8517	0.6596	0.8384

CONCLUSION

The boundary layer nanofluid flow under microgravity environment near a stagnation point is sucessfully studied with different types and shapes of nanoparticles. The fluid problem was mathematically formulated into a system of partial differential equation and solved numerically. The detail of the effect analysed are as follows;

1. The increase of nanoparticle volume fraction increases temperature profile, skin friction coefficient and Nusselt number but decrease in term of velocity profile.
2. Alumina nanoparticle has the highest velocity profile while copper nanoparticle has the highest temperature profile, skin friction coefficient and Nusselt number.

3. Sphere shape of nanoparticles has the highest velocity profile but blade shape of nanoparticles has thicker boundary layer thickness.
4. Blade shape nanoparticles has the highest velocity and skin friction coefficient compared with other nanoparticles.
5. Cylinder shape of nanoparticles has the highest Nusselt number.

ACKNOWLEDGEMENT

The authors would like to acknowledge the Ministry of Higher Education Malaysia and Research Management Centre UTM, Universiti Teknologi Malaysia (UTM) for financial support through vote numbers FRGS/1/2019/STG06/UTM/02/15 and 08G33.

REFERENCES

[1] C. Maxwell, James, *A treatise on electricity and magnetism*. London and Edinburg: Oxford-Clarendon Press, 1873.
[2] S. U. S. Choi, *Enhancing thermal conductivity of fluids with nanoparticles* in American Society of Mechanical Engineers, Fluids Engineering Division (Publication) FED, 1995.
[3] S. U. S. Choi, Z. G. Zhang, W. Yu, F. E. Lockwood, and E. A. Grulke, "Anomalous thermal conductivity enhancement in nanotube suspensions," Appl. Phys. Lett., vol. 79, no. 14, pp. 2252–2254, 2001.
[4] K. Khanafer, K. Vafai, and M. Lightstone, "Buoyancy-driven heat transfer enhancement in a two-dimensional enclosure utilizing nanofluids," Int. J. Heat Mass Transf., vol. 46, no. 19, pp. 3639–3653, 2003.
[5] R. K. Tiwari and M. K. Das, "Heat transfer augmentation in a two-sided lid-driven differentially heated square cavity utilizing nanofluids," Int. J. Heat Mass Transf., vol. 50, no. 9–10, pp. 2002–2018, 2007.
[6] R. Jmai, B. Ben-Beya, and T. Lili, "Heat transfer and fluid flow of nanofluid-filled enclosure with two partially heated side walls and different nanoparticles," Superlattices Microstruct., vol. 53, no. 1, pp. 130–154, 2013.
[7] M. Zubair, Z. Shah, S. Islam, W. Khan, and A. Dawar, "Study of three dimensional Darcy–Forchheimer squeezing nanofluid flow with Cattaneo–Christov heat flux based on four different types of nanoparticles through entropy generation analysis," Adv. Mech. Eng., vol. 11, no. 5, pp. 1–17, 2019.
[8] Z. Hajabdollahi, H. Hajabdollahi, and K. C. Kim, "Multi-objective optimization of solar collector using water-based nanofluids with different types of nanoparticles," J. Therm. Anal. Calorim., vol. 140, no. 3, pp. 991–1002, 2020.
[9] F. S. Javadi *et al.*, "The effects of nanofluid on thermophysical properties and heat transfer characteristics of a plate heat exchanger," Int. Commun. Heat Mass Transf., vol. 44, pp. 58–63, 2013.
[10] M. M. Elias, I. M. Shahrul, I. M. Mahbubul, R. Saidur, and N. A. Rahim, "Effect of different nanoparticle shapes on shell and tube heat exchanger using different baffle angles and operated with nanofluid," Int. J. Heat Mass Transf., vol. 70, pp. 289–297, 2014.
[11] M. Sheikholeslami and M. M. Bhatti, "Forced convection of nanofluid in presence of constant magnetic field considering shape effects of nanoparticles," Int. J. Heat Mass Transf., vol. 111, pp. 1039–1049, 2017.
[12] R. Ellahi, M. Hassan, and A. Zeeshan, "Shape effects of nanosize particles in Cu-H2O nanofluid on entropy generation," Int. J. Heat Mass Transf., vol. 81, pp. 449–456, 2015.
[13] I. Khan, "Shape effects of MoS2 nanoparticles on MHD slip flow of molybdenum disulphide nanofluid in a porous medium," J. Mol. Liq., vol. 233, pp. 442–451, 2017.
[14] A. Zaraki, M. Ghalambaz, A. J. Chamkha, M. Ghalambaz, and D. De Rossi, "Theoretical analysis of natural convection boundary layer heat and mass transfer of nanofluids: Effects of size, shape and type of nanoparticles, type of base fluid and working temperature," Adv. Powder Technol., vol. 26, no. 3, pp. 935–946, 2015.
[15] N. Bachok, A. Ishak, R. Nazar, and I. Pop, "Flow and heat transfer at a general three-dimensional stagnation point in a nanofluid," Phys. B Condens. Matter, vol. 405, no. 24, pp. 4914–4918, 2010.
[16] M. Mustafa, T. Hayat, I. Pop, S. Asghar, and S. Obaidat, "Stagnation-point flow of a nanofluid towards a stretching sheet," Int. J. Heat Mass Transf., vol. 54, no. 25–26, pp. 5588–5594, 2011.
[17] A. Malvandi, F. Hedayati, and D. D. Ganji, "Slip effects on unsteady stagnation point flow of a nanofluid over a stretching sheet," Powder Technol., vol. 253, pp. 377–384, 2014.
[18] T. Hayat, M. I. Khan, M. Waqas, A. Alsaedi, and M. Farooq, "Numerical simulation for melting heat transfer and radiation effects in stagnation point flow of carbon – water nanofluid," Comput. Methods Appl. Mech. Eng., vol. 315, pp. 1011–1024, 2017.
[19] F. A. Soomro, R. U. Haq, Q. M. Al-Mdallal, and Q. Zhang, "Heat generation/absorption and nonlinear radiation effects on stagnation point flow of nanofluid along a moving surface," Results Phys., vol. 8, pp. 404–414, 2018.
[20] M. J. Uddin, W. A. Khan, and A. I. Ismail, "g-Jitter induced magnetohydrodynamics flow of nanofluid with constant convective thermal and solutal boundary conditions," PLoS One, vol. 10, no. 5, pp. 1–15, 2015.
[21] N. A. Rawi, A. R. M. Kasim, Z. M. Isa, A. Mangi, and S. Shafie, "g-Jitter effects on the mixed convection flow of nanofluid past an inclined stretching sheet," Front. Heat Mass Transf., vol. 8, no. 12, pp. 1–7, 2017.
[22] N. A. Rawi, M. R. Ilias, Z. Mat Isa, and S. Shafie, "Effect of gravity modulation on mixed convection flow of second grade fluid with different shapes of nanoparticles," Malaysian J. Fundam. Appl. Sci., vol. 13, no. 2, pp. 132–136, 2017.
[23] M. H. A. Kamal, N. A. Rawi, A. Ali, and S. Shafie, "Effects of g-jitter and radiation on three-dimensional double diffusion stagnation point nanofluid flow," Appl. Math. Mech. (English Ed.), vol. 41, no. 11, pp. 1707–1722, 2020.
[24] M. H. A. Kamal, A. Ali, S. Shafie, N. A. Rawi, and M. R. Ilias, "g-Jitter effect on heat and mass transfer of 3D stagnation point nanofluid flow with heat generation," Ain Shams Eng. J., vol. 11, no. 4, pp. 1275–1294, 2020.
[25] F. R. Hamdan *et al.*, "g-Jitter free convection flow near a three-dimensional stagnation-point region with internal heat generation," *J. Adv. Res. Fluid Mech. Therm. Sci.,* vol. 67, no. 1, pp. 119–135, 2020.
[26] I. Waini, A. Ishak, and I. Pop, "Dufour and Soret effects on Al2O3-water nanofluid flow over a moving thin needle: Tiwari and Das model," Int. J. Numer. Methods Heat Fluid Flow, vol. 31, no. 3, pp. 766–782, 2021.
[27] R. Ellahi, M. Hassan, and A. Zeeshan, "Shape effects of spherical and nonspherical nanoparticles in mixed convection flow

over a vertical stretching permeable sheet," Mech. Adv. Mater. Struct., vol. 24, no. 15, pp. 1231–1238, 2017.
[28] E. V. Timofeeva, J. L. Routbort, and D. Singh, "Particle shape effects on thermophysical properties of alumina nanofluids," J. Appl. Phys., vol. 106, no. 1, 2009.
[29] I. Waini, A. Ishak, and I. Pop, "Nanofluid flow on a shrinking cylinder with Al_2O_3 nanoparticles," Mathematics, vol. 9, no. 14, pp. 1–13, 2021.
[30] S. Shafie, "Mathematical Modelling of g-Jitter Induced Free Convection," Universiti Teknologi Malaysia, 2005.